Characterizing tissue with acoustic parameters derived from ultrasound data

P. Littrup[a], N. Duric[b], R. R. Leach Jr.[c], S. G. Azevedo[c], J. V. Candy[c], T. Moore[c], D. H. Chambers[c], J. E. Mast[c], E. Holsapple[a]
[a]Karmanos Cancer Institute, 110 East Warren Ave, Detroit MI 48201, [b]Department of Physics and Astronomy, University of New Mexico, [c]Lawrence Livermore National Laboratory

ABSTRACT

In contrast to standard reflection ultrasound (US), transmission US holds the promise of more thorough tissue characterization by generating quantitative acoustic parameters. We compare results from a conventional US scanner with data acquired using an experimental circular scanner operating at frequencies of 0.3 – 1.5 MHz. Data were obtained on phantoms and a normal, formalin-fixed, excised breast. Both reflection and transmission-based algorithms were used to generate images of reflectivity, sound speed and attenuation.. Images of the phantoms demonstrate the ability to detect sub-mm features and quantify acoustic properties such as sound speed and attenuation. The human breast specimen showed full field evaluation, improved penetration and tissue definition. Comparison with conventional US indicates the potential for better margin definition and acoustic characterization of masses, particularly in the complex scattering environments of human breast tissue. The use of morphology, in the context of reflectivity, sound speed and attenuation, for characterizing tissue, is discussed.

Keywords: ultrasound imaging, tissue characterization, acoustic parameters, breast cancer.

1. INTRODUCTION

The Karmanos Cancer Institute is developing an ultrasound device for measuring and imaging acoustic parameters of human tissue. The device has been developed to the engineering prototype stage and has been used to perform a variety of experiments. This paper discusses the experimental results relating to tissue characterization, that is, the use of ultrasound (US) to identify and quantify various tissue types, with a specific focus on diagnosing breast cancer. The overall goal of the project described herein, is improved tissue characterization of breast masses and reliable detection of abnormal microcalcifications found in some breast cancers and ductal carcinoma in situ (DCIS). Current breast US is limited to mass evaluation, whereas mammography also detects and guides biopsy of malignant calcifications. Neither approach provides quantitative tissue identification.

Improved tissue characterization could result in a reduction of the estimated one million benign biopsies performed each year in the United States[1], costing up to several billion dollars[2]. Most breast calcifications are benign and comprise ~ 80% of stereotactic biopsies guided by mammography[3]. Ultrasound has the capability of finding some groups of calcifications[4-6], but further improvements in resolution should also address tissue characterization to define the soft tissue filling of ducts by DCIS. In this manner, CURE may be able to more accurately identify the malignant calcifications associated with progression of DCIS or early cancers.

Currently, high-resolution US images of the breast are performed in the reflection mode at relatively high frequencies (roughly 5 – 15 MHz). Reconstruction of reflection ultrasound images relies upon acoustic impedance differences in the tissue and includes only direct backscatter of the ultrasound signal. Resolution and tissue contrast of current US continues to improve with denser transducer arrays and better image processing but direct tissue characterization remains elusive.

2. MATERIALS AND METHODS

The initial technical goal of the CURE program was to provide sub-millimeter resolution and quantitative tissue characterization using both reflection and transmission US. To that end, the Karmanos Cancer Institute (KCI) contracted with the Lawrence Livermore National Laboratory (LLNL) to build an engineering prototype capable of acquiring 3-D US data. LLNL was also tasked with developing the initial algorithms for image reconstruction. The engineering prototype and some of the initial results are described in a previous paper[7]. Additional algorithms are being developed in collaboration with physicists at Groupvelocity, LLC. The associated image reconstructions are being used to test the feasibility of characterizing tissue, as described below.

2.1 The Data

Data were acquired by scanning two phantoms and a cadaveric breast. Two basic phantoms were used to model mass margins and punctate resolution (i.e., cyst and microcalcifications). The "cyst" phantom consisted of a 4 cm diameter cylinder containing uniform US-scattering agar and two smaller cylinders, each 1 cm in diameter, separated from each other and imbedded in the agar. The smaller cylinders contained a water-alcohol mixture with a lower sound speed than the surrounding agar. In this manner, the cylinders mimicked the slower sound speed in fluid filled cysts in a low contrast setting. A second phantom (henceforth the "calcification" phantom) consisted of a 4-cm diameter cylinder containing ten, 0.2-mm diameter nylon strings embedded through the cylinder at a fixed radius. The strings were grouped into five pairs with separations ranging from two to five mm within each pair. The third target consisted of a normal cadaveric breast placed in formalin and sealed in a 10-cm diameter, cylindrical container.

The two phantoms and cadaveric breast specimen were scanned by the CURE scanner at a frequency of 1.5 MHz using 2 microsecond pulses. The relatively low frequency of 1.5 MHz was used in order to better penetrate the phantoms and broaden the beam angle while retaining sub-mm spatial resolution. The receivers and transmitters were positioned along a ring trajectory having a diameter of 20 cm. A total of 1280 receiver positions and 320 transmitter positions were used, corresponding to lambda/4 and lambda spacing, respectively. Each target was placed at the center of the ring with the long axis of the cylinder oriented vertically relative to the plane of the ring. Each data set represents a 2-D slice through the phantom. The ring plane could be translated in the vertical direction allowing for 3-D reconstructions from stacked 2-D planes of data. The phantoms were also scanned with a clinical reflection ultrasound unit (GE Logiq 600) and a clinical CT scanner (GE Lightspeed Quad detector array). The former was used for comparing image quality while the latter was used to establish the "truth" images. The CT scans were performed at 1.25 mm slice thickness. All CURE scans were performed at 10 millimeter slice thickness to generate multiple tomographic images per phantom.

2.2 The Algorithms

Acquiring the data is only the first step leading to tissue characterization. Producing quantitative ultrasound images requires the ability to accurately model the physics of US pulse propagation in tissue. In this study, the acoustic properties of sound speed, attenuation and reflectivity were determined and imaged using a family of algorithms. The algorithms are grouped into two basic types and are described below.

Reflection Algorithms:

Our full aperture tomography (FAT) algorithm allows circumferential processing of reflection and transmission data. An extension of reflection mode imaging, or so-called "B-scans" currently used in medical ultrasound, FAT produces images that highlight scattering sources in the insonified object. It assumes the wave scattering is isotropic and sound speed in the medium is known or calculable. The method is analogous to synthetic aperture radar (SAR) or delay-and-sum beam forming techniques[8]. FAT models the object to be imaged as a collection of point scatterers. A linearizing assumption is made that acoustic energy scattered by each individual point object does not scatter off other point scatterers. This assumption of ignoring multiple scattering allows one to formulate the imaging solution for a single point scatterer independent of all other point scatterers. Then, the solution involving all point scatters becomes the linear superposition of the result from each individual point scatterer. The scattered signal from a given point in the object is

sampled around the aperture (circular or paddle geometry) scanned by the receiving transducer. Assuming the point scatters isotropically, it effectively becomes a secondary point source. Thus, the goal of the imaging method is to determine the location of the point source given the data collected around the aperture.

Transmission Algorithms:

Straight-Ray/Bent_ray Algorithm: The simplest implementation of an image reconstruction algorithm ignores scattering and assumes that the ultrasound pulses travel in straight lines. This is the essential assumption behind X-ray CT reconstructions. Sound speed information is extracted on the basis of arrival time differences. Attenuation is determined on the basis of the strength (amplitude) of the arriving signal relative to the departing signal. More sophisticated versions of the algorithm allow for multiple scatterings (bent-ray). Both types of algorithms are being developed. Early results from these algorithms are described in a previous paper[7].

Diffraction Algorithm: This algorithm is built around the assumption that all scattering is weak (e.g. Bourne approximation). However, in regions of strong scattering, the approximation fails, resulting in strong artifacts. The diffraction tomography algorithm (DT) used in this study is built upon the work by Devaney[9] and Andre[10] and others. DT produces quantitative sound parameter images when the scattered field is sufficiently sampled relative to a wavelength. This technique includes the mathematics of diffraction using Born or Rytov models, but does not include strong scattering models. The DT method we use is performed largely in the Fourier domain with a final transform into the spatial image domain. Like FAT, DT is a single step process, with no iteration, so it can be performed reasonably quickly. It produces quantitative images of sound speed and attenuation.

Full Wave Algorithm: The most sophisticated algorithms implement full or nearly full solutions to the acoustic wave equation. Measurements of the phase and amplitude of the scattered field are used to reconstruct the properties of the medium. Examples and descriptions of such algorithms can be found in Johnson et al[11] and Natterer et al[12]. These algorithms are potentially the most accurate though they tend to be slower than the simpler codes because of the extra computational burden. The algorithm used in this study is the one described in Johnson et al[11].

3. RESULTS

We now describe and discuss the images obtained by applying the above algorithms to the data acquired with the CURE scanner. The discussion of the results is grouped according to the type of target used (see section 2.1 for a description of the targets).

The microcalcification phantom. Figure 1 shows three images of the microcalcification phantom. The main intent of this experiment was to demonstrate the ability to detect features smaller than the resolution of the instrument. Figure 1a shows the image obtained with a conventional B-scan operating in the 6-11 MHz range. Each of the compact objects is 0.2 mm. It is obvious that the B-scan image can pick out these small objects. The strong reflecting boundary of these objects offsets their smaller size. The usual speckle and shadow artifacts can be seen. Figure 1b shows an image of the same phantom "slice" made with the CURE prototype operating at 1.5 MHz. This reconstruction was made using a full aperture (data collected along a ring surrounding the phantom) reconstruction. The improved point definition and separation of the features can be attributed to the multiple views inherent to the CURE approach. Furthermore, the absence of speckle artifacts can be attributed to the lower operating frequency of 1.5 MHz. The enhanced sensitivity to reflectivity suggests that it may be possible to improve characterization of microcalcifications using only their strong reflection signatures. Figure 1c is an image made from the transmission data using a full wave algorithm. This image shows adequate point separation and ability to quantify sub-millimeter regions. Furthermore it demonstrates the higher sound speed values associated with the "microcalcifications" mimicked by nylon in the case of the phantom.

The cyst phantom. The standard B-scan reflection ultrasound image (Figure 2a) shows the characteristic "cystic", or anechoic, appearance of the fluid cylinders. These have a sharp leading edge, but limited lateral and posterior wall definition. The usual speckle, glint and shadow artifacts can be seen. Figure 2b shows a CURE reflection image at 1.5 MHz reconstructed with a full aperture tomography (FAT) reflection algorithm. Despite the low frequency, the margins of the "cysts" are crisply defined throughout their circumference and show improved detail. One cylinder contained an involuted segment, whereas the other cylinder had an exophytic linear region corresponding to an adjacent crack in the agar. These cylinder contours were not as well defined by the standard B-scan image due to its dependence on

transducer position and assumption of only 180 degree backscatter. The absence of major artifacts can be attributed to the lower operating frequency and the multiple views. Figure 2c and 2d are transmission images which confirm the lower attenuation and sound speed (i.e., darker centers) of the cylinder contents. The attenuation image made by our diffraction algorithm (Figure 2c) still shows more of the cylinder contour detail than standard US, but some contour artifacts are produced at the margins of strong scattering. The sound speed image (Figure 2d) was reconstructed using a full wave algorithm and demonstrates lower sound speed within the cylinder than the adjacent agar. These subtle attenuation and sound speed differences are of comparable magnitude to the differences between cyst fluid and adjacent normal breast tissue.

Excised Breast. Figure 3a shows an X-ray CT image generated with 1.25 mm slice thickness through the normal breast specimen showing predominantly fatty tissue with only thin internal fibrous bands. Figure 3b is a standard B-scan ultrasound image of the specimen. Showing. Figure 3c is the CURE image obtained at 1.5 MHz in which the reflection and transmission data are simply overlayed and contains no additional post-processing to enhance tissue detail. The CURE image shows the overall specimen configuration with excellent morphologic comparison to the CT scan. There is also no loss of signal or resolution seen in the near or far field. Despite the low frequency of the CURE image, the fine architectural detail of internal fibrous bands is similar to the CT image (the latter was made at a thinner slice thickness and resultant high radiation exposure). Tissue characterization of ultrasound parameters was not directly correlated with any histologic section, but the background sound speed pattern matches the overall fatty appearance on the CT scan. The grey scale represents varying speeds. The whitest portions represent a sound speed of about 1450 m/s. The darkest regions have speeds of about 1550 m/s.

4. DISCUSSION

The feasibility of submillimeter resolution ultrasound with potential tissue characterization by sound parameters has been demonstrated for the engineering prototype phase of the CURE program. These goals were also confirmed in a complex scattering medium of cadaveric human breast tissue. The potential benefits for clinical breast imaging are improved tumor margin visualization and characterization. We now discuss the potential for characterization using morphology based on reflectivity, sound speed and attenuation.

Reflectivity: Breast tissue characterization by current reflection US may be best represented by the success of the 'Stavros/Colorado' criteria for mass margin evaluation[13]. The 98% accuracy obtained for defining a benign mass rested upon the criterion of an ovoid mass with well-defined margins. This was sufficient for ATL, Inc. to obtain separate Food and Drug Administration approval for characterizing benign breast masses with their high-resolution transducer in 1996[14]. Compound imaging[15] produces a single averaged image from 3-9 single angled scans, reducing speckle, clutter and ultrasound artifacts. Mass margins are thus better identified[16]. However, little clinical progress has been noted for additional US tissue characterization to improve breast tissue diagnosis. The CURE images (Figures 1b, 2b and 3c) suggest that mass margin definition may be greatly expanded when evaluated using multiple views, and perhaps in 3 dimensions. CURE identification of clear mass margins therefore does not suffer from the need for tumor capsules[5,13] to be discretely identified as specular reflectors, nor from incomplete lateral margins from diffraction artifacts. Our "cyst" phantom clearly demonstrated improved margin evaluation for both reflection and transmission algorithms. The possibility for three-dimensional evaluation of all aspects of tumor mass may hold great promise for improved tissue characterization by simple morphology.

Sound Speed: Images of sound speed are shown in Figures 1c, 2d and 3c. In the case of the microcalcification phantom (Figure 1c), the increase in sound speed at the locations of the nylon strings is distinct and obvious with the sound speed rising from a background level of 1510 m/s to over 1700 m/s. These results demonstrate the ability to define sound speed variations for small sub-wavelength objects and the potential to help characterize microcalcifications. The sound speed image of the cyst phantom demonstrates the ability to detect more subtle variations in sound speed (Figure 2d). The drop in sound speed in the interiors of the "cysts" is indicative of the water-alcohol mixture that these small cylinders contain. The drop is quantified to be 15 m/s relative to the background agar. This result suggests that it may be possible to characterize cysts on the basis of their sound speed morphology. Finally, the sound speed image of the cadaveric breast is shown in Figure 3c. Unfortunately, a full-wave reconstruction of this target is not available. We show instead a simple

straight-ray reconstruction. Despite its relative simplicity the image shows well-defined variations in the sound speed, ranging from 1450 m/s to over 1550 m/s. This range of sound speed is consistent with known variations in sound speed for the breast. The lower range represents fatty tissue while the higher range represents ducts and muscle tissue. Inspection of figure 3c shows that the fibrous bands are embedded within tissue with sound speed lower than water. Sound speeds in the medium range from 1450 to 1500 m/s below that of water. Comparison with data from the visible woman project suggests that, on the basis of sound speed alone, the medium is that of fatty breast tissue. A priori knowledge of the excised breast confirms that this specimen is a fatty breast. Some enhancement of the sound speed in regions where the fibrous bands are concentrated is also evident. Such an enhancement is expected since fibrous tissue and ductal tissues have sound speed higher than fat. We acknowledge that further tissue correlation studies are warranted and were not the focus of this feasibility study.

Attenuation: We have not yet concentrated much effort on reconstruction of attenuation. For completeness we note the attenuation image shown in Figure 2c. This image of the cyst phantom was obtained with the diffraction algorithm. It is evident that there is a distinct difference in the attenuation properties of the small liquid-filled cylinders relative to the agar. We have not yet attempted to quantify this difference and this work remains for the future.

The greatest potential benefit of tissue characterization is the ability to discriminate accurately between cancerous and non-cancerous tissue. It is unlikely that any one acoustic parameter will do the job. The most likely path to such diagnostic capability entails comparisons of multiple acoustic parameters (e.g. et al)[17]. For example, in the case of the microcalcification phantom, the reflectivity data alone only shows that there exist features with strongly reflecting surfaces. The sound speed data alone only shows that the features have higher sound speed. The combination suggests that the features are highly reflective *and* have higher sound speed a characterization that points to microcalcifications as opposed to soft tissue. Similarly, the combined acoustic properties of the cyst phantom (reflectivity showing the walls, sound speed showing the decrease in sound speed and the difference in attenuation) point to a liquid-filled cyst *without the need to interpret artifacts*. Finally, in the case of the cadaveric breast the combined sound speed and reflectivity data are actually shown superimposed in figure 3. The combined information (when compared to the X-ray CT scan) increases the characterization of the breast tissue by identifying the fatty tissues and the fibrous bands. The use of multi-parameter characterization (data fusion) is discussed in a separate paper in these proceedings.

5. CONCLUSIONS AND FUTURE WORK

It has been shown that the combination of angular diversity (multiple views) and good image reconstruction algorithms can yield high quality US images with great potential for characterizing tissue. The use of relatively simple phantoms has demonstrated the potential for using acoustic parameters to characterize microcalcifications and liquid-filled cysts. In the case of real breast tissue there is promise for characterization based on reflectivity and sound speed. The work described herein is ongoing. Future work will concentrate on better sound speed reconstructions of breast tissue and reconstructions of attenuation to complement the use of sound speed and reflectivity in a multi-parameter study of tissue characterization.

6. ACKNOWLEDGMENTS

The authors would like to acknowledge the support of several individuals in this work. They are Michael Berggren of Techni-Scan, Inc., for the use of their phantoms and for their reconstructions, Dr. John Boone at U. C. Davis Medical center for the X-ray CT images and Dr. Alex Babkin and Prof. Robert Duncan (University of New Mexico) for their help with the image reconstructions. Funding for this project was provided by philanthropic support of the Karmanos Cancer Institute.

7. REFERENCES

1. Liberman L. Clinical management issues in percutaneous core breast biopsy. Radiol Clin North Am. 2000; 38:791 807.
2. Secker-Walker RH, Vacek PM, Hooper GJ, Plante DA, Detsky AS. Screening for breast cancer: time, travel, and out-of-pocket expenses. J Natl Cancer Inst 1999, 91:702-8.
3. Makoske T, Preletz R, Riley L, Fogarty K, Swank M, Cochrane P, Blisard D. Long-term outcomes of stereotactic breast biopsies. Am Surg. 2000, 66:1104-8.
4. Cleverley JR, Jackson AR, Bateman AC. Pre-operative localization of breast microcalcification using high-frequency ultrasound. Clin Radiol. 1997; 52:924-6.
5. Skaane P. Ultrasonography as adjunct to mammography in the evaluation of breast tumors. Acta Radiol Suppl. 1999; 420:1-47.
6. Teh WL, Wilson AR, Evans AJ, Burrell H, Pinder SE, Ellis IO. Ultrasound guided core biopsy of suspicious mammographic calcifications using high frequency and power Doppler ultrasound. Clin Radiol. 2000; 55:390-4.
7. Littrup, P. et al. Computerized Ultrasound Risk Evaluation (CURE) System: Development of Combined Transmission and Reflection Ultrasound with New Reconstruction Algorithms for Breast Imaging. To appear in the proceedings of the 26th International Acoustical Imaging Symposium: Windsor, Canada. September 9-12, 2001.
8. Fitch, J. P., *Synthetic Aperture Radar*, Springer-Verlag, 1988.
9. A. J. Devaney. A filtered backpropagation algorithm for diffraction tomography. Ultrasonic Imaging, 4(4):336-350, October 1982.
10. André MP, Janee HS, Martin PJ, Otto GP, Spivey BA, Palmer DA. High-speed data acquisition in a diffraction tomography system employing large-scale toroidal arrays. International Journal of Imaging Systems and Technology 1997; 8:137-147.
11. S. A. Johnson and M. L. Tracy. Inverse scattering solutions by a sinc basis, multiple source, moment method. Part I: Theory, Ultrasonic Imaging, 5:361-375, 1983.
12. Natterer, F. A Propagation-Backpropagation Method for Ultrasound Tomography, Inverse Problems 11, 1225-1232, 1995.
13. Stavros AT, Thickman D, Rapp CL, Dennis MA, Parker SH, Sisney GA. Solid breast nodules: use of sonography to distinguish between benign and malignant lesions. Radiology. 1995;196:123-34.
14. 61 Federal Register 60712-60713 (1996). (http://www.rsna.org/REG/research/regulatory/wfprfcexamples.html).
15. Entrekin RR, Porter BA, Sillesen HH, Wong AD, Cooperberg PL, Fix CH. Real-time spatial compound imaging application to breast, vascular, and musculoskeletal ultrasound.Semin Ultrasound CT MR 2001 Feb;22(1):50-64
16. Shapiro RS, Simpson WL, Rausch DL, Yeh HC. Compound spatial sonography of the thyroid gland: evaluation of freedom from artifacts and of nodule conspicuity. AJR Am J Roentgenol 2001 Nov;177(5):1195-8
17. Schreiman JS, Gisvold JJ, Greenleaf JF, Bahn RC. Ultrasound transmission computed tomography of the breast. Radiology 1984; 150:523-30.

(a) (b) (c)

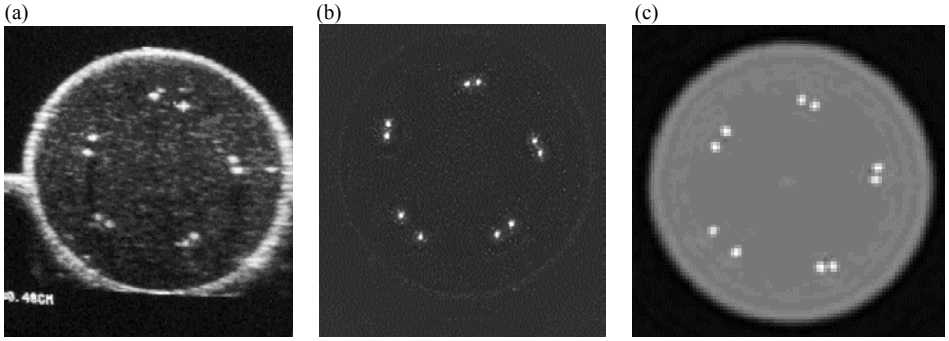

Figure 1. (a) B-Scan image of the "calcification" phantom. (b) Full aperture reflection image. (c) Sound speed reconstruction using the full wave algorithm (calculated by TechniScan, Inc.)". Phantom furnished by TechniScan Inc.

(a) (b)

(c) (d)

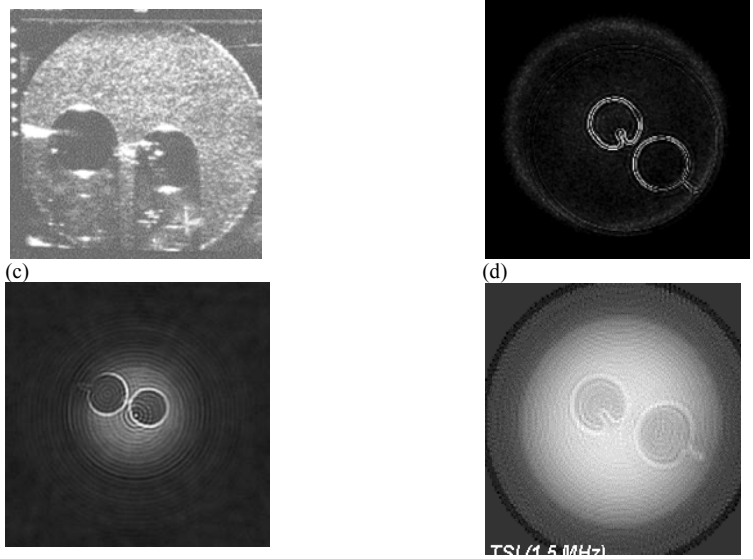

Figure 2. (a) The B-scan image of the "cyst" phantom. (b) The full aperture reflection image. (c) The attenuation image from the diffraction algorithm. (d) The sound speed image using the full wave algorithm (calculated by TechniScan Inc). Phantom furnished by TechniScan Inc.

(a)

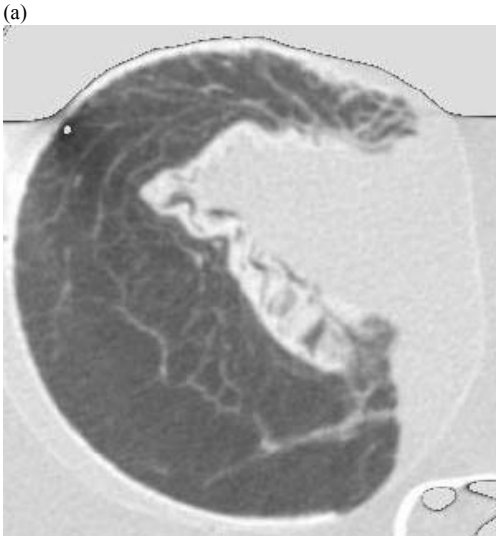

(b)

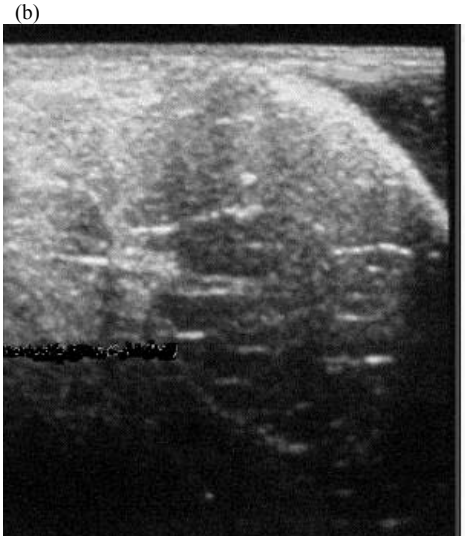

(c)

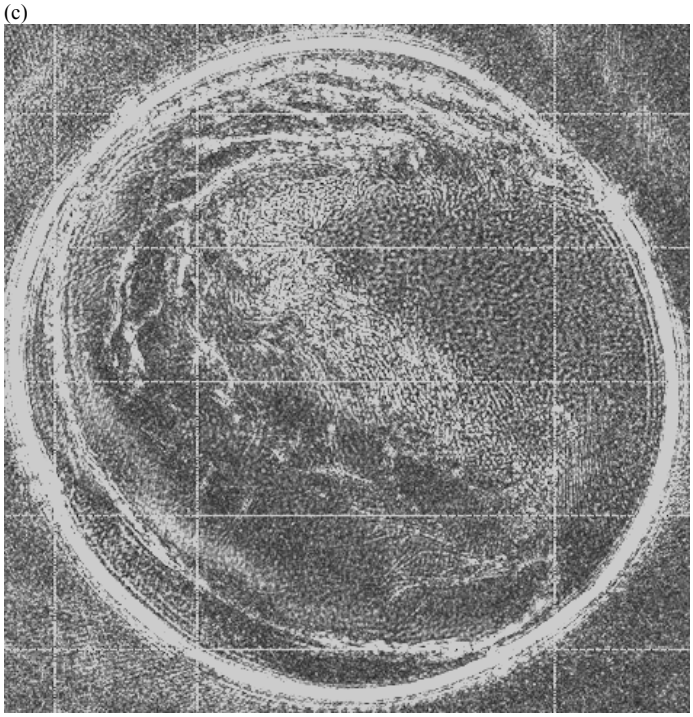

Figure 3. (a) X-Ray CT scan of cadaveric breast. (b) B-Scan of a portion of the breast. (c) Reflection image superimposed on a sound-speed reconstruction. Cadaveric breast courtesy of TechniScan Inc.